Research in Astron. Astrophys. **2010** Vol. **10** No. **3**, 244–252
http://www.raa-journal.org *http://www.iop.org/journals/raa*

Research in Astronomy and Astrophysics

The study of proto-magnetar winds

Yan-Jun Chen[1] and Ye-Fei Yuan[2]

[1] Department of Physics and Electronic Science, Changsha University of Science and Technology, Changsha, Hunan 410114; *chenyjy@ustc.edu.cn*
[2] Center for Astrophysics, University of Science and Technology of China, Hefei 230026, China

Received 2009 April 27; accepted 2009 October 25

Abstract The velocity profiles and properties of proto-magnetar winds are investigated. It is found that the corotation of wind matter with magnetic field lines significantly affects r-process nucleosynthesis and could lead to long duration γ-ray bursts and hyper-energetic supernovae.

Key words: stars: neutron — stars: winds, outflows — supernovae: general — stars: magnetic fields — nuclear reactions, nucleosynthesis, abundances

1 INTRODUCTION

According to nucleosynthesis theory (Burbidge et al. 1957), most heavy elements with charge number $Z > 30$ are formed in neutron-capture (n-capture) processes. In spite of their tiny abundances in Solar system matter ($\sim 10^{-6}\%$), n-capture elements can produce obvious spectral line absorptions, and thus are detectable in many astronomical observables, such as the metal-poor Galactic halo stars. These processes are defined as a slow process (s-process) if the timescale for neutron capture is much longer than the decay timescale and a rapid process (r-process) when the situation is reversed for unstable nuclei. Modern studies indicate that s-process and r-process elements have different origins. In fact, theoretical studies have led to the identification of the s-process site in low- to intermediate-mass stars (i.e., $M \sim 1.3 - 8\,M_{\odot}$) during the red giant phase, specifically the asymptotic giant branch (AGB) stage (Zhang et al. 1996, 2006). However, the actual astrophysical site for the r-process has not been identified so far. Sneden et al. (2008) showed that the observed abundances of n-capture elements in metal-poor star CS 22892–052 reproduce the r-process curve of the solar system remarkably well. This suggests a universal range of conditions for the r-process of the universe. It is known that for the r-process to be effective, it needs the ratio of neutrons to seed nuclei to be greater than 100. This fact limits the matter specific entropy, electron fraction and dynamic timescale of the physical process in a stringent region. The nascent neutron star neutrino-driven wind, due to the appropriate dynamic timescale and richness in neutrons, is considered one of the most promising sites to investigate the r-process (Qian & Wasserburg 2007).

It is well known that most neutron star formation results from the core collapse of the end-stage evolution of a massive star accompanied by supernova (SN) explosions (Burrows 2000). Although the detailed mechanism is still elusive, a great deal of theoretical research and numerical simulations indicate that the gravitational binding energy is carried away predominantly by all species of neutrinos. A fraction of neutrino energy is absorbed by the surface layers of the proto-neutron stars (PNSs) and the surrounding atmosphere, and on timescales ≤ 1 s after core collapse, heats the material below

the stalled shock to result in a SN re-explosion; at $t \geq 1$ s, it continues heating the cavity evacuated by the SN shock and drives material from the star's surface to form a persistent thermal wind with photons, electrons, positrons, nucleons, α particles and some heavy elements trapped in it. The wind continues blowing for about the neutrino-diffusing timescale in a PNS, i.e., the Kelvin-Helmholtz cooling epoch, lasting for $10 \sim 100$ s.

Although the PNS winds are one of the promising sites for effective r-process nucleosynthesis, as yet, unfortunately, none of the theoretical models are entirely capable of successfully reproducing the abundances of r-process elements seen in nature (Qian & Wasserburg 2007). One of the promising schemes is to consider the PNSs with very strong magnetic fields, i.e., proto-magnetars. Recent investigations (Metzger et al. 2007, 2008) based on the MHD analysis indicate that strong magnetic fields favor the appearance of the effective r-process, but require several stringent conditions. However, their conclusions are reached in the framework of non-relativity. Cardall & Fuller (1997) and Otsuki et al. (2000), dedicated to the study of non-magnetic winds, showed that general-relativistic (GR) effects can provide favorable conditions for the r-process to be effective. Moreover, though the origin of large magnetic strengths is not very clear, Duncan & Thompson (1992) argued that it is due to an efficient dynamo by the stellar core's millisecond rotation at birth that magnetars develop $\sim 10^{15}$ G magnetic fields. Such rapid rotation and high magnetic fields have dramatic consequences for the dynamics of the PNS winds. First, a neutron star with a millisecond spin period has a reservoir of rotational energy on the scale of a SN explosion. Secondly, the strong magnetic field lines force the wind matter to corotate which provides an efficient mechanism for spindown. Therefore, the proto-magnetar winds may drive a hyper-energetic SN or be the central engine of long-duration GRBs (Thompson et al. 2004).

The above review stimulates the present work. In addition, it is known that near the surface of a PNS, the density ρ is about on the scale 10^{10} g cm^{-3} and the temperature $T \sim 5$ MeV, therefore the thermal pressure $P = 11\pi^2 T^4/180 + \rho T/m_{\rm n} \sim 10^2$ MeV cm^{-3}. When $B \geq 10^{15}$ G, the magnetic energy density $B^2/(8\pi) \geq 10^2$ MeV cm^{-3}. If the magnetic energy density is comparable to or larger than the thermal pressure, the magnetic fields will significantly contribute to or dominate the dynamics of the wind. In the present work, to highlight the influence of the magnetic field on the winds, we use the magnetic field strength of the PNS's surface $B_0 = 10^{15}$ G as one paradigm for investigation. In view of the fact that it is also the characteristic magnetic field strength of a magnetar, we believe that it is a reasonable choice. This work is organized as follows. In Sections 2 and 3, we briefly describe the formulae for evaluating the proto-magnetar wind properties in Newtonian and GR form and give the inputs and numerical method used in this paper. The results are presented in Section 4. Conclusions are given in Section 5.

2 THE FORMULAE

2.1 The Newtonian Winds

As proposed by Weber & Davis (1967) and Michel (1969), in this work, for a time-independent neutrino-driven MHD wind, we only consider all physical quantities restricted to the equatorial plane (but still assumed to have spherical symmetry) and omit their θ components. The time-independent non-relativistic MHD equations for flow are

$$\dot{M} = 4\pi r^2 \rho v_{\rm r} \ , \tag{1}$$

$$\mathcal{L} = \mathcal{L}_{\rm gas} + \mathcal{L}_{\rm mag} = r v_\phi - \frac{r B_{\rm r} B_\phi}{4\pi \rho v_{\rm r}} \ , \tag{2}$$

$$I = r(v_\phi B_{\rm r} - v_{\rm r} B_\phi) \ , \tag{3}$$

$$v_{\rm r}\frac{dv_{\rm r}}{dr} = \frac{v_\phi^2}{r} - \frac{1}{\rho}\frac{dP}{dr} - \frac{GM}{r^2} - \frac{1}{4\pi\rho}\Big(\frac{B_\phi^2}{r} + B_\phi \frac{dB_\phi}{dr}\Big) \ . \tag{4}$$

In this steady state, $\mathcal{L}$ is the specific angular momentum, and I is the so called "consequence of induction." Conservation of magnetic flux requires the total magnetic flux, $\Phi_B = r^2 B_{\rm r}$ to be constant in radius. The wind energy and entropy equations are

$$\frac{dE}{dr} = \frac{q_\nu}{v_{\rm r}} \ , \qquad T\frac{ds}{dr} = \frac{q_\nu}{v_{\rm r}} \ , \tag{5}$$

where E is defined as

$$E = \frac{1}{2}(v_{\rm r}^2 + v_\phi^2) + h - \tilde{\alpha} - \frac{r\Omega v_{\phi{\rm A}} v_{\rm A}}{v_{\rm r}}, \tag{6}$$

in which $v_{\phi{\rm A}} = B_\phi/(4\pi\rho)^{1/2}$ and $v_{\rm A}$ is the Alfvén speed defined as $v_{\rm A} = B_{\rm r}/(4\pi\rho)^{1/2}$, h is the specific enthalpy and $\tilde{\alpha}$ is defined as $\tilde{\alpha} = M/r$. The energy deposition rate per unit mass q_ν provides a source term in the above equations and is related to the reactions for the charged-current processes $\nu_{\rm e} + {\rm n} \leftrightarrow {\rm p} + {\rm e}^-$ and $\bar{\nu}_{\rm e} + {\rm p} \leftrightarrow {\rm n} + {\rm e}^+$, inelastic neutrino-lepton, -baryon scattering and the process $\nu\bar{\nu} \leftrightarrow {\rm e}^+{\rm e}^-$. In this paper, we use the rates obtained by Thompson et al. (2001). Combining the above equations, one can obtain the logarithmic derivative of the velocity as

$$\frac{d\ln v_{\rm r}}{dr} = \frac{t_1}{t_2} \ , \tag{7}$$

where the expression of t_1 will be given as

$$t_1 = \xi_1\frac{dE}{dr} + \xi_2\frac{ds}{dr} + \xi_3\frac{d\tilde{\alpha}}{dr} + \xi_4\frac{1}{r} + \xi_5\frac{d\ln B_{\rm r}}{dr} \ , \tag{8}$$

with $\tilde{\alpha} = M/r$. Here ξ_i values are given respectively by

$$\begin{aligned}
\xi_1 &= (1-x^2)^2 \ , \\
\xi_2 &= -(1-x^2)^2\frac{\partial h}{\partial s} \ , \\
\xi_3 &= (1-x^2)^2 \ , \\
\xi_4 &= [R^2\Omega^2(1-2x^2) + \frac{\mathcal{L}^2}{r^2}x^4] \ , \\
\xi_5 &= (1-x^2)[x^2 v_{\phi{\rm A}}^2 - (1-x^2)c_{\rm s}^2] \ ,
\end{aligned}$$

where $\partial h/\partial s = T + D/C_V$, C_V is the specific heat and $D = (T/\rho)(\partial P/\partial T)_\rho$. Also, t_2 is given as

$$\begin{aligned}
t_2 &= (1-x^2)^2\Big(v_{\rm r}^2 - c_{\rm s}^2 + \frac{x^2}{1-x^2}v_{\phi{\rm A}}^2\Big) \\
&= -\frac{(1-x^2)}{v_{\rm A}^2}(v_{\rm r}^2 - v_{\rm SM}^2)(v_{\rm r}^2 - v_{\rm FM}^2) \ ,
\end{aligned} \tag{9}$$

where $x^2 = v_{\rm r}^2/v_{\rm A}^2$ and slow-magnetosonic (SM) and fast-magnetosonic (FM) velocities are defined as

$$v_{\rm SM}^2 = K - \sqrt{K^2 - c_{\rm s}^2 v_{\rm A}^2} \ , \tag{10}$$

$$v_{\rm FM}^2 = K + \sqrt{K^2 - c_{\rm s}^2 v_{\rm A}^2} \ , \tag{11}$$

where $K = (v_{\rm A}^2 + c_{\rm s}^2 + v_{\phi{\rm A}}^2)/2$ and $c_{\rm s}$ is the speed of sound.

2.2 The General-Relativistic Winds

In Schwarzschild spacetime, the dynamics of the winds are governed by the equations

$$T^{\alpha\beta}_{\ \ ;\beta} = \rho q^{\alpha}, \tag{12}$$

$$F^{\alpha\beta}_{\ \ ;\beta} = 4\pi J^{\alpha}, \tag{13}$$

$$F_{[\alpha\beta;\gamma]} = F_{[\alpha\beta,\gamma]} = F_{\alpha\beta,\gamma} + F_{\beta\gamma,\alpha} + F_{\gamma\alpha,\beta} = 0. \tag{14}$$

The corresponding quantities to those in the Newtonian wind are

$$\dot{M} = 4\pi r^2 \rho u_p \alpha \ , \qquad \Phi_B = r^2 B_{\rm r} \alpha \ , \tag{15}$$

$$\mathcal{L} = hrv_\phi y - \frac{\alpha R B_\phi B_{\rm r}}{4\pi\rho u_p} \ , \tag{16}$$

$$I = r\alpha(\alpha v_\phi B_{\rm r} - v_{\rm r} B_\phi) \ , \tag{17}$$

with $\alpha = \sqrt{1-2M/r}$. The equivalent functions for the wind entropy and energy respectively are

$$\frac{dE}{dr} = \frac{q_\nu/y}{u_p} \ , \qquad T\frac{ds}{dr} = \frac{q_\nu/\alpha}{u_p} \ , \tag{18}$$

where u_p is defined as $u_{\rm r}/\alpha$ with $u_{\rm r}$ being the radial component of the fluid 4-velocity, $v_{\rm r}(= u_p/y)$ is the corresponding 3-velocity, $y = \sqrt{(1+u_p^2)/(1-v_\phi^2)}$ and

$$E = h\alpha y - \frac{\alpha R\Omega B_\phi B_{\rm r}}{4\pi\rho u_p} \ . \tag{19}$$

From the above, we obtain

$$\frac{d\ln u_p}{dr} = \frac{t_1}{t_2} \ , \tag{20}$$

where the expression of t_1 will be given as

$$t_1 = \xi_1 \frac{dE}{dr} + \xi_2 \frac{ds}{dr} + \xi_3 \frac{d\ln\alpha}{dr} + \xi_4 \frac{1}{r} + \xi_5 \frac{d\ln B_{\rm r}}{dr} \ , \tag{21}$$

where ξ_i values are given respectively by

$$\xi_1 = (k_0 - x^2)\Big[(E-\Omega\mathcal{L})(k_0 - 2x^2) + \Big(\frac{E}{\alpha^2}\Big)x^4\Big] \ ,$$

$$\xi_2 = -\Big[(k_0 - x^2)(k_2 x^2 + k_4 x^4) + (k_0 - 2x^2)f\Big]\frac{\partial \ln h}{\partial s} \ ,$$

$$\xi_3 = (k_0 - x^2)\Big[k_2\alpha^2 - \Big(\frac{E}{\alpha}\Big)^2 x^4\Big] - 2\alpha^2 f \ ,$$

$$\xi_4 = (k_0 - x^2)\Big[\Big(\frac{\mathcal{L}}{r}\Big)^2 x^4 - k_2 r^2\Omega^2\Big] + 2r^2\Omega^2 f \ ,$$

$$\xi_5 = \frac{(k_0 - x^2)(k_2 x^2 + k_4 x^4) - (k_0 c_{\rm s}^2 - x^2 c_{\rm s}^2 + x^2)f}{1 + c_{\rm s}^2} \ ,$$

where $x^2 = u_p^2/u_{\rm A}^2$ with $u_{\rm A} = B_{\rm r}/(4\pi\rho h)^{1/2}$, and $\partial \ln h/\partial s = T/h + D/C_V$, and $D = T/(e + P)(\partial P/\partial T)_\rho$. Moreover, $c_{\rm s}$ is the sound 4-velocity defined by $c_{\rm s}^2 = a_{\rm s}^2/(1-a_{\rm s}^2)$ with $a_{\rm s}^2$ being given

by $a_{\rm s}^2 = (\partial \ln h/\partial \ln \rho)_{\rm s}$, and

$$k_0 = \alpha^2 - r^2\Omega^2 ,$$
$$k_2 = \Big(E - \Omega\mathcal{L}\Big)^2 ,$$
$$k_4 = \Big(\frac{\mathcal{L}}{r}\Big)^2 - \Big(\frac{E}{\alpha}\Big)^2 ,$$

and $f = k_2(k_0 - 2x^2) - k_4 x^4$, and t_2 is

$$t_2 = \frac{h^2(k_0 - x^2)^3}{1 + c_{\rm s}^2}\Big(u_p^2 - c_{\rm s}^2 + \frac{x^2}{k_0 - x^2}u_{\phi{\rm A}}^2\Big)$$
$$= -\frac{h^2(k_0 - x^2)^2}{(1 + c_{\rm s}^2)u_{\rm A}^2}(u_p^2 - u_{\rm SM}^2)(u_p^2 - u_{\rm FM}^2) , \quad (22)$$

where $u_{\phi{\rm A}} = B_\phi/(4\pi\rho h)^{1/2}$, and

$$u_{\rm SM}^2 = K - \sqrt{K^2 - k_0 c_{\rm s}^2 u_{\rm A}^2} , \quad (23)$$
$$u_{\rm FM}^2 = K + \sqrt{K^2 - k_0 c_{\rm s}^2 u_{\rm A}^2} , \quad (24)$$

where $K = (k_0 u_{\rm A}^2 + c_{\rm s}^2 + u_{\phi{\rm A}}^2)/2$. Compared with the Newtonian SM and FM velocities given by Equations (10) and (11), the general-relativistic equivalence Equations (23) and (24) are identical except for k_0.

3 INPUTS AND NUMERICAL METHOD

In this work, we use $1.4\,M_\odot$ and 10 km as the representative PNS mass and radius. The neutrino reaction rates are taken to be the same as those of Thompson et al. (2001). The neutrino luminosities are scaled as $L_{\nu_{\rm e}} = L_{\bar\nu_{\rm e}}/1.3 = 1.8L_{\nu_\mu}$, where μ denotes each of the other four species of neutrinos and antineutrinos. The average neutrino energies are scaled with luminosities as $\langle E_\nu\rangle \propto L_\nu^{1/4}$, with $[\langle E_{\nu_{\rm e}}\rangle, \langle E_{\bar\nu_{\rm e}}\rangle, \langle E_{\nu_\mu}\rangle]$ at [11, 14, 23] MeV for $L_{\bar\nu_{\rm e}} = 8\times10^{51}$ erg s^{-1}. We do not consider the sub-magnetosonic wind. Therefore, the outflow velocity passes smoothly through the SM, Alfvén and FM critical points in sequence. This situation is more complicated than in the case of non-magnetic wind (Thompson et al. 2001), which has one critical point, i.e., the sonic point. As indicated by Equations (9) and (22), when the outflow velocity matches the wave velocity of the SM and FM wave modes, the denominator of Equations (7) and (20) becomes zero; to ensure continuity of the solution through the SM and FM critical points, the numerator must simultaneously be zero. In order to solve Equations (7) and (20), we must also know the uncertain mass outflow rate and also determine the two unknown critical radii $r_{\rm SM}$ and $r_{\rm FM}$. The shooting method, as one of the methods to solve the ordinary differential equation, is inappropriate for Equations (7) and (20). For this reason, we use another method in this article, the so called relaxation algorithm, which is described in the textbook (Press et al. 1992) in detail.

4 RESULTS

Figure 1 presents the velocities as functions of radius for GR and Newtonian winds. As discussed above, the chosen surface magnetic field strength makes the PNS wind magnetically dominated. Therefore, the large centrifugal force results in a great enhancement of the outflow speed (at large radius $\sim 0.75c$), compared with the non-magnetic (NM) wind (at large radius $\sim 0.1c$). The discrepancy between the GR and Newtonian results for the outflow speed is small and due to the appearance

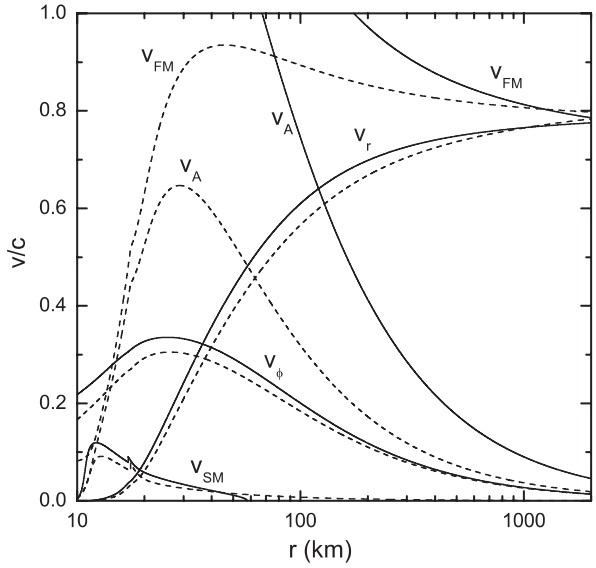

Fig. 1 Velocities as functions of radius for general relativistic (*solid lines*) and Newtonian (*dashed lines*) winds.

of α particles; the magnetosonic velocities all show a discontinuity, especially for $v_{\rm SM}$ at $r \sim 18\,$km. Note that the GR-type $v_{\rm A}$ and $v_{\rm FM}$ exceed light speed in a range of radii, but there is no trouble because they do not cause physical signals.

As indicated by Hoffman et al. (1997), a successful r-process for achieving all abundance peaks requires

$$\frac{(S^{\rm a})^3}{\tau_{\rm dyn}} \gtrsim F \ , \tag{25}$$

where $S^{\rm a}$ denotes the asymptotic entropy of the outflow and F is only a function of the asymptotic electronic fraction $Y_{\rm e}^{\rm a}$. The dynamical timescale $\tau_{\rm dyn}$ is defined as

$$\tau_{\rm dyn} \equiv \left[\frac{\rho}{u_{\rm r}|d\rho/dr|}\right]_{T=0.5\,{\rm MeV}} \ . \tag{26}$$

Firstly, we show that $S^{\rm a}$ and $\tau_{\rm dyn}$ are functions of the stellar rotation period P in the left and right panels in Figure 2, respectively. It is shown that the GR effects on $\tau_{\rm dyn}$ are not important except for very short periods (left panel), while those on $S^{\,\rm a}$ are significant (right panel). These phenomena can be partially understood by the small discrepancy between the velocity profiles for Newtonian and GR winds in Figure 1 and by the comparison of the equations for the outflow entropy s in Equations (5) and (18), from which we can see that the factor α in Equation (18) coming from the Schwarzschild geometry at small radii obviously affects the dynamic equation of s (similar discussion can be applied to temperature T), resulting in a greater GR wind calculation of $S^{\,\rm a}$ than for the Newtonian one. Notice that the exponent of $S^{\,\rm a}$ is 3 in Equation (25), so the appropriate change of $S^{\rm a}$ can lead to the distinct variation of the left-hand side of Equation (25). Moreover, $S^{\,\rm a}$ is seen to drop when the rotation period decreases due to the great speed of the wind pushed by the large centrifugal force which means that the outflow does not have enough time to be heated. Also, one sees that weaker neutrino luminosity results in greater $S^{\,\rm a}$. $S^{\rm a}$ can be approximately given by

$$S^{\rm a} \simeq S^{\rm a}_{\rm NM} \exp(-\Omega/\Omega_S) \ , \tag{27}$$

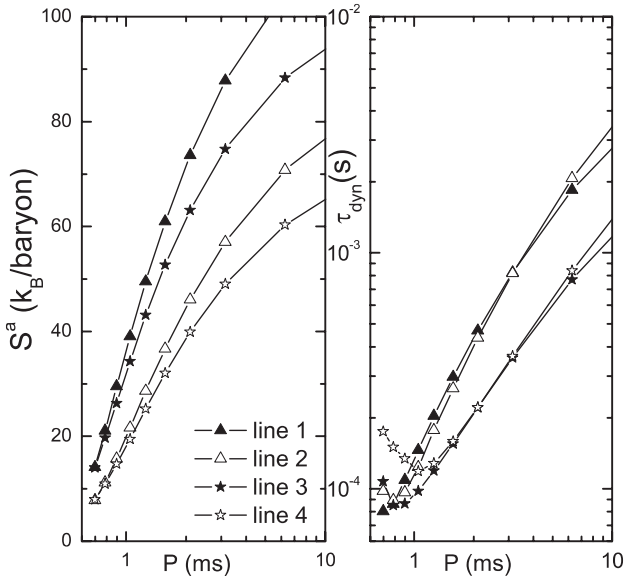

Fig. 2 Asymptotic specific entropy $S^{\rm a}$ (*left panel*) and dynamical timescale $\tau_{\rm dyn}$ (*right panel*) as functions of rotation period P. Lines 1 and 3 are for the GR cases while lines 2 and 4 are for the Newtonian ones. Pentacles are for $L_{\bar{\nu}_{\rm e}} = 8 \times 10^{51}$ erg s^{-1} and triangles are for 3.5×10^{51} erg s^{-1}.

where $\Omega_S \simeq \Omega_0 (L_{\bar{\nu}_{\rm e},51}/8)^{0.1}$ and $S^{\rm a}_{\rm NM} \simeq S_0 (L_{\bar{\nu}_{\rm e},51}/8)^{-0.2}$ with $\Omega_0 = 4000$ and $S_0 = 80$ for the Newtonian form and 4800 and 110 for the GR one. For $\tau_{\rm dyn}$, as shown in Equation (26), there are two factors which affect it. One is the scale height of the wind density, i.e., $|d\rho/dr|/\rho$, the other is the outflow velocity $u_{\rm r}$. The rotational effects make $u_{\rm r}$ increase, thus decreasing $\tau_{\rm dyn}$, while for the most rapidly rotating solution, the centrifugal support is sufficient to expand the scale height of the wind at small radii, which results in the increase of $\tau_{\rm dyn}$ for Newtonian calculations. Note that the large GR effects at small radii significantly cancel out this increase.

The left side of Equation (25) is shown as a function of P in Figure 3. Compared with the NM results, one can see that strong magnetic fields really favor the r-process. In the strong magnetic fields, Figure 2 shows that the rotational effects decrease $\tau_{\rm dyn}$ in most cases favoring the r-process and the decreasing $S^{\rm a}$ disfavors the r-process. Competition between these factors results in the best situations for a successful r-process for $P \approx 2 - 3$ ms. Moreover, we found that considering GR effects, the successful r-process would take place more easily in PNS winds with strong magnetic fields, consistent with the conclusions (Cardall & Fuller 1997; Otsuki et al. 2000) for the NM case.

Figure 4 depicts the mass loss rates as a function of P. One sees that due to the large centrifugal force, for $P \lesssim 3$ ms, the mass loss rates $\dot{M}$ rapidly grow. Empirically, $\dot{M}$ is given by

$$\dot{M} \simeq \dot{M}_{\rm NM} \exp[(\Omega/\Omega_{\dot{M}})^2] \ , \tag{28}$$

where $\dot{M}_{\rm NM}$ is the mass loss rate for NM winds and $\Omega_{\dot{M}} \approx \Omega_0 (L_{\bar{\nu}_{\rm e},51}/8)^{0.04}$ s^{-1} with $\Omega_0 = 3500$ for the Newtonian form and 4300 for the GR one. The total angular momentum loss rate is $\dot{J} = \mathcal{L}\dot{M}$; therefore, the rotational power loss is $\dot{E}_{\rm rot} = \Omega \dot{J}$. For PNS with initial rotation period $P_0 \approx 1$ ms, the rotational energy is about 2×10^{52} erg. If we assume the neutrino luminosity drops linearly with PNS evolution time as Metzger et al. (2007) did, the rotational power loss is $\dot{E}_{\rm rot} \gtrsim 5 \times 10^{51}$ erg during the Kelvin-Helmholtz epoch, about 1/4 of the rotational energy, which is consistent with the energy required to produce long duration γ-ray bursts and hyper-energetic supernovae.

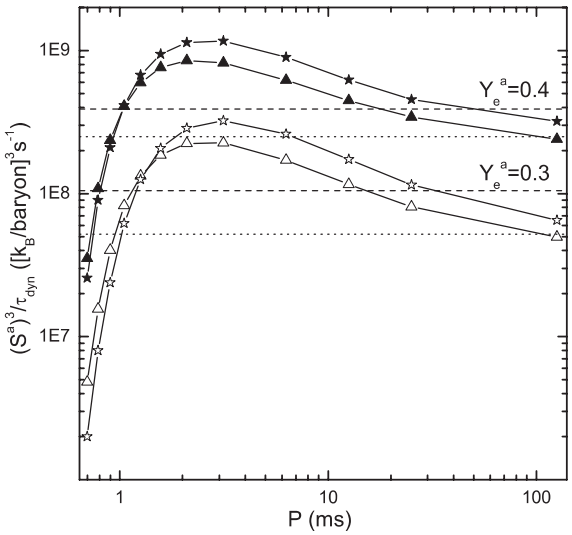

Fig. 3 $(S^{\rm a})^3/\tau_{\rm dyn}$ as a function of the rotation period P. Curves are the same as in Fig. 2. Dashed lines are the critical values above which the successful r-process is achieved for two demonstrated values of $Y_{\rm e}^{\rm a}$. Dotted lines are for the non-magnetic calculations.

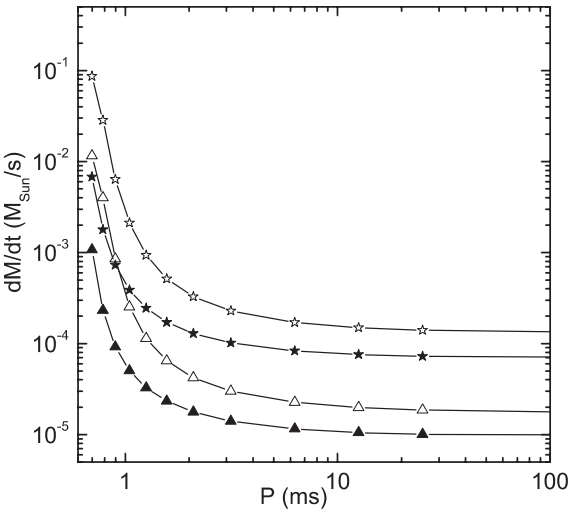

Fig. 4 Mass loss rates as a function of P. Curves are the same as in Fig. 2.

5 CONCLUSIONS

In summary, we have investigated the velocity profiles and properties of proto-magnetar winds for both Newtonian and general relativistic forms in this paper. The corotation of the wind material with the magnetic field lines makes the outflow speed and mass loss rate increase and reduces the asymptotic entropy and dynamical timescale. Our calculations show that $P \approx 2-3$ ms is the most effective in successful r-process generation for the Newtonian and general relativistic cases and, considering

the general relativistic effects, nucleosynthesis can successfully occur in proto-magnetar winds. The extracted energy is sufficient for producing long duration γ-ray bursts and hyper-energetic supernovae. However, conclusions will only be ultimately reached after more detailed studies. This work is in progress.

Acknowledgements This work is supported by the National Basic Research Program of China (2009CB824800) and the research grants of Changsha University of Science and Technology.

References

Burbidge, E. M., Burbidge, G. R., Fowler, W. A., et al. 1957, Rev. Mod. Phys., 29, 547
Burrows, A. 2000, Nature, 403, 727
Cardall, C. Y., & Fuller, G. M. 1997, ApJ, 486, L111
Duncan, R. C., & Thompson, C. 1992, ApJ, 392, L9
Hoffman, R. D., Woosley, S. E., & Qian, Y. Z. 1997, ApJ, 482, 951
Metzger, B. D., Thompson, T. A., & Quataert, E. 2007, ApJ, 659, 561
Metzger, B. D., Thompson, T. A., & Quataert, E. 2008, ApJ, 676, 1130
Michel, F. C. 1969, ApJ, 158, 727
Otsuki, K., Tagoshi, H., Kajino, T., et al. 2000, ApJ, 533, 424
Press, W. H., Teukolsky, S. A., Vetterling, W. T., & Flannery, B. P. 1992, Numerical recipes in C: The Art of Scientific Computing (Cambridge, MA: Cambridge Univ. Press) (*http://www.numerical-recipes.com*)
Qian, Y. Z., & Wasserburg, G. J. 2007, Phys. Rep., 442, 237
Sneden, C., Cowan, J. J., & Gallino, R. 2008, Annu. Rev. A&A, 46, 241
Thompson, T. A., Burrows, A., & Meyer, B. S. 2001, ApJ, 562, 887
Thompson, T. A., Chang, P., & Quataert, E. 2004, ApJ, 611, 380
Weber, E. J., & Davis, L. J. 1967, ApJ, 148, 217
Zhang, B., Chang, R. X., & Peng, Q. H. 1996, Progress in Astronomy, 14(4), 275 (in Chinese)
Zhang, B., & Cui, W. Y. 2006, Progress in Astronomy, 24(1), 54 (in Chinese)